www.georesursy.ru

ORIGINAL ARTICLE

DOI: https://doi.org/10.18599/grs.2026.1.7

Main Mechanisms of Lake Evolution of Hilganta and Gorbunka (Southeastern Transbaikalia)

S.V. Borzenko[*], *I.A. Komogortseva*

Institute of Natural Resources, Ecology, and Cryology of the Siberian Branch of the Russian Academy of Sciences, Chita, Russian Federation

Abstract. The article examines the hydrogeochemical history of continental saline, chloride lakes Hilgant and Gorbunka, located in the southeast of Transbaikalia. Brief information is given on the composition of host rocks and the chemical composition of water involved in the salt supply to the lakes. The mineral and chemical compositions, values of the isotopic ratios of carbon and oxygen of carbonates in different layers of lake bottom sediments are described. Indicator minerals are distinguished that characterize different climatic conditions. The main conditions are identified that characterize the content and ratios of the main chemical components and pH during changes in the salinity of lake water. Based on ^{210}Pb measurements, the current rate of sediment accumulation in the lakes is calculated. Thermodynamic calculations analyzing water evaporation and under-ice water concentration are discussed. The possibility of forming authigenic minerals is considered. Ultimately, the geochemical evolution of the lakes is interpreted in relation to regional climate changes in the recent past.

Keywords: saline lakes, authigenic and chemogenic minerals, evolution.

Recommended citation: Borzenko S.V., Komogortseva I.A. (2026). Main Mechanisms of Lake Evolution of Hilganta and Gorbunka (Southeastern Transbaikalia). *Georesursy = Georesources*, 28(1), pp. 160–176. https://doi.org/10.18599/grs.2026.1.7

Introduction

In recent years, the issue of salt lake evolution has become a subject of increased interest mainly due to climate change (Donchyts et al., 2016; Erler et al., 2018; Yechieli et al., 2002; Maberly et al., 2020, Solotchin et al., 2021; Maltsev et al., 2022), as they are considered more representative for understanding patterns in transformation of their biological component, water chemical composition and mineral content of sediments because of relatively rapid changes in hydrological parameters compared to freshwater lakes (Khotinsky, 1977; Velichko, 1989, 2012; Subetto, 2009; Jones et al., 2009; Tweed et al., 2011; Boros et al., 2014; Deocampo, Jones, 2014; Mianping, 1997). The most promising reconstructions of geochemical evolution directions of lakes are sedimentary sections of bottom deposits that record even minor environmental changes (Warren, 1989; Strakhov, 1993; Zheng, 2014 etc.).

In Russia, modern research on diagenetic processes is mainly focused on large water bodies such as lakes in Karelia and Western Siberia (Bezrukova et al., 2017; Gaskova et al., 2017; Leonova et al., 2018; Kolpakova et al., 2020 and others), while smaller water bodies receive less attention (Strakhovenko et al., 2010; Sklyarov et al., 2010, 2017; Solotchina et al., 2013; Solotchin et al., 2017), and there are only isolated publications concerning the lakes of South-Eastern Transbaikalia (Bazarova et al., 2011; Zamana et al., 2011). In recent decades, much attention has been paid to authigenic carbonate minerals and layered silicates of lake bottom sediments, whose structural characteristics and quantitative ratios in the section of lake deposits change significantly in response to changes in natural environment and regional climate (Solotchina, 2009; Solotchina et al., 2017; Solotchin et al., 2024 and others). By alternating “cold” and “warm” associations of layered silicates, fluctuations in biogenic silica content, (Ca, Mg)-carbonates and a number of other features in the sections studied by these authors, climatic intervals responsible for changing hydrochemical indicators of lakes have been identified. In this regard, solving problems related to the genesis of different chemical

[*]Corresponding author: Svetlana V. Borzenko
e-mail: svb_64@mail.ru

types of lakes can be achieved through identification of paragenetic associations composition of chemical elements and minerals, sequence of their formation and accumulation in sections of lacustrine deposits.

The aim of this work was to identify geochemical markers in bottom sediments of small lakes existing under identical landscape-climatic and geological-geochemical conditions, as well as to detect the relationship between authigenic and chemogenic mineral formation with transformation of lake chemical composition due to climate changes.

Research methods

This message presents the results of hydrochemical studies conducted on Lake Hilganta and Lake Gorbunka in different years. Chemical analysis measurements of water samples were carried out using standard methods. Calcium and magnesium concentrations were determined by atomic absorption method in argon-acetylene flame using a SOLAAR 6M spectrophotometer. The sodium and potassium content was measured by flame emission method. Potentiometric methods were used to determine pH, Eh, Cl^-. Titration was applied for determining total dissolved inorganic carbonate concentration (TDIC = CO_3^{2-} + HCO_3^-). Sulfate ion was analyzed turbidimetrically. Microcomponent composition of waters and chemical composition of sediments were determined by ICP-MS method.

Undisturbed sediment cores were sampled in accordance with the requirements of GOST 17.1.5.01-80. Polypropylene tubes 100 cm long with an internal diameter of 4.5 cm were used as sampling devices. Each sample was divided into layers depending on the nature of the sediment (color, density, presence of any inclusions). The results of X-ray structural analysis of the mineral composition of lake bottom sediments were obtained using powder diffraction method at the National Research Tomsk State University and the Shared Use Center "Geodynamics and Geochronology" of the Earth Crust Institute SB RAS. XRD measurements were performed on a DRON-4 instrument equipped with an automated powder diffractometer (CuKα radiation, graphite monochromator). Diffractograms were scanned over the range of 2θ from 3° to 65° with a step size of 0.05°, scanning time per point 4 s, slit width 0.5 mm.

To study the chemical composition and element fractionation in bottom sediments, a modified sequential extraction procedure of Tessier was used (Table 1) (Tessier et al., 1979). Bottom sediment samples were first dried to air-dry state and ground in jasper mortar (particle size 75 μm). The mass of sediment taken for analysis was 2 g. Between extraction stages, the residue was washed with distilled water, dried again, and sample weight was re-fixed. In addition to extracted fractions, total contents of chemical elements were measured.

To determine the water surface area of lakes, images from the Landsat TM, ETM+, and OLI satellites with a resolution of 30 m and processing level Level1 were used. The data was obtained using the Earth Explorer service (http://earthexplorer.usgs.gov/). Processing of satellite imagery and calculation of water indices were carried out using the tools in ArcGIS 10's Image Classification and Spatial Analyst modules. To clarify the physicochemical conditions for formation of chemogenic minerals, thermodynamic modeling of processes in the system water–rock was conducted. Modeling was performed using the PHREEQC software (Parkhurst, Appelo, 2013). Physicochemical calculations were done using Pitzer's database for highly mineralized waters (Pitzer, 1992). For assessing the degree of saturation of waters by minerals, the saturation index (Q/K) was calculated, whose values become positive at supersaturation (lgQ – lgK > 0.3), while ±0.3 characterizes equilibrium between solution and mineral (Pačes, 1983).

Research object

The lakes are located in the northern part of the Daurian ecoregion, in a hilly steppe zone on the watershed between the Onon and Aga rivers at an altitude of 660–670 m above sea level, 250 km southeast of Chita. The lakes are endorheic with water surface area up to 0.5 km² and shallow (average depth ~0.5 m). Hydrological characteristics of the lakes are subject to significant chronological changes. The reason for such variations is fluctuations in climatic conditions causing periodic filling and drying out of the lakes. Changes in lake water levels can be inferred from terraces formed at heights ranging from 0.5 to 2 meters observed in

Stage	Fraction	Extractant	Time and temperature
A	Exchangeable	1M KNO_3, pH=7, V = 20 mL	T=25ºC, t=5 h
B	Bound to Oxides and Carbonates	0.04 M NH_4OH·HCl in 25% HOAc, V = 20 mL	T=96ºC, t=2 h (microwave)
C	Bound to Organic Matter	0.02 M HNO_3 V = 5 mL + 30% H_2O_2 V = 8 mL, pH 2	T=85ºC, t=1 h (microwave)
		3.2 M NH_4OAc in 20% HNO_3 V = 7 mL	T=25°C, t=30 min
D	Residual	1 portion 65% HNO_3 + 3 portion 32 % HCl, V = 20 mL	T = 220 °C, t = 1 h

Table 1. Stages of sequential extraction

the basins of Lake Gorbuinka and Lake Hilganta respectively. According to data (Obyazov, 2007), long-term fluctuations in atmospheric precipitation reveal intra-century cycles lasting from 8–10 to 35 years. The first decade of this century has been characterized as arid in the region, marked by the driest climate over the past two hundred years. According to the same author, the sharp increase in aridity was caused by superimposition of lower atmospheric moisture content onto higher air temperatures compared to those of the preceding period.

In the seasonal dynamics of hydrological regime of lakes there are also significant differences. These differences are due to semi-arid sharply continental climate with cold long winter and short warm summer. The warm period with stable positive temperatures in this region averages 190–200 days (from April 10–15 to October 23–27). Annual precipitation amount, most of which falls during the summer season (80%), is on average equal to 340 mm, which is almost two times lower than evaporation rate. Water temperature in summer fluctuates from 18 to 24 °C, while air temperature below −15 °C lasts for about 80–85 days. During winter, lakes freeze through to their bottoms, and a layer of gudzhir (salts) forms on ice surface. Strong winds scatter gudzhir across steppe areas. When ice melts, lakes refill again with water.

Snowless winters and sharp temperature fluctuations lead to intensive leaching of rocks represented by Quaternary alluvial deposits (sands, gravels, etc.) consisting of non-crystallized volcanic glass forming the main mass (up to 20%), plagioclase (up to 70%) and pyroxenes (up to 10%). Among accessory minerals magnetite is found (up to 5%). Secondary minerals are quartz, chlorite, clay material and iron hydroxides. Terrigenous material enters lakes mainly through temporary rain flows from drainage areas. Atmospheric precipitation, groundwater and summer storm runoff are the primary income components of lake water balance, while evaporation from the lake surface represents its major expenditure component. Precipitation falling on lake catchment areas belongs to ultra-fresh waters (total dissolved solids – TDS = 10–50 mg/L), slightly acidic (pH 5–6.5), mostly HCO_3 Ca type. Groundwaters are also fresh (TDS < 1 g/L), pH 7.0–8.5, predominantly HCO_3 Ca-Mg type (Borzenko et al., 2020).

Results of study

Lake waters

The analysis of satellite images obtained using Landsat TM, ETM+, and OLI instruments showed that between 2004 and 2014 the lakes reached relatively low surface areas (Fig. 1), which coincided with particularly low average atmospheric precipitation amounting to 225 mm per year. In contrast, relatively large lake surfaces were observed during a period of high water levels from 1980 to 1999, corresponding to an annual precipitation rate of 370 mm.

The studied lakes belong to the rare Cl Na type for this region (Borzenko, 2021). According to our epizootic observations conducted between 2008 and 2022, salinity in Hilganta Lake varied from 8 to 36 g/L, while pH values ranged from 8.07 to 8.33 (Table 2).

Observations made over Gorbunka Lake from 2008 to 2022 indicated its water salinity fluctuated within limits of 7 to 184 g/L, with pH ranging from 7.47 to 8.49. Maximum salinity was recorded in both lakes during the driest year (2014), when their surface area was minimal (Fig. 1).

Relatively lower water salinity in these lakes was noted at the beginning of territory humidification periods (in 2018 and 2021). Overall, chloride ions dominated as the main anion in lake waters (74–91 eq%), followed by sodium cations among cations (77–95 eq%). The second most important anion by chemical equivalents was sulfate (9–21 eq%). Relative content of total dissolved inorganic carbon did not exceed 6 eq%. Among cations magnesium was the second most significant component, varying from 4 to 20 eq%,

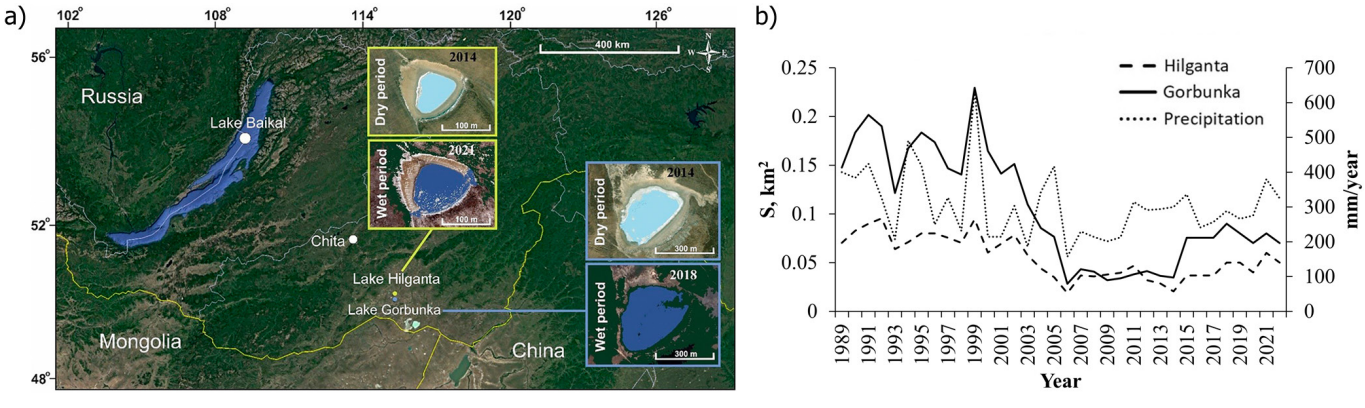

Fig. 1. Scheme showing locations and areas of Hilganta and Gorbunka lakes (a) depending on atmospheric precipitation amount (b). (Data from Federal State Budgetary Institution "Zabaykalskoye Upradleniye po gidrometeorologii i monitoringu okruzhayushchey sredy" (Zabaykalsky Hydrometeorological Monitoring Agency)

Parameters		Gorbunka							Hilganta				
	Date	2008-07-18	2013-07-10	2014-07-01	2018-07-06	2020-07-11	2021-07-04	2022-07-13	2008-07-06	2013-07-04	2014-07-06	2020-07-10	2022-07-14
Eh	mV	0	190	42.3	115	150	15	-116	123	29	66.5	-80.6	-3
pH		8.18	8.08	7.47	8.49	8.00	7.52	8.33	8.07	8.17	8.07	8.33	8.16
TDIC	mg/L	304	161	124	441	163	119	380	276	255	206	369	247
SO_4		6472	2148	14758	671	2522	6120	1663	6042	2110	3647	1316	3064
Cl		18984	12018	100291	3368	14430	37060	7225	15642	6212	13657	3723	7906
Ca		18.6	59.1	160	31.4	19.4	27.1	29.7	99.5	62.9	54.1	23.2	69.9
Mg		681.5	468.1	3794.6	120.3	229.1	915.7	416.1	1408.1	509.8	895.3	352.7	702.4
Na		14720	7830	65000	2315	10171	24865	4704	10157	4047	8871	2435	5145
K		77.6	103.5	237.6	38.3	38	121.9	48.8	94.1	60.1	41	29.1	49
TDS*	g/L	41	23	184	7	28	69	14	36	13	27	8	17
Li	µg/L	400.00	312.35	1470.00	12.00	76.96	82.64	37.29	106.14	82.10	185.96	32.21	45.29
Se		52.00	40.30	191.00	20.00	42.00	85.00	4.18	1.20	1.15	1.24	0.20	0.50
Br		70233	61824	368587	33250	136508	211960	52778	166188	34489	80625	36220	64027
Rb		6.52	4.81	24.97	1.23	6.48	6.63	2.81	7.09	4.32	5.46	2.18	4.14
Sr		4230	3625	18506	1231	2797	3035	1442	7208	2863	5743	1105	3217
U		18.23	15.59	58.95	0.21	0.43	0.33	0.57	0.82	0.08	1.07	1.98	0.42
rMg/rCa	-	61	13	40	6	20	56	23	24	14	28	25	17
rSr/rCa		0.227	0.061	0.116	0.039	0.144	0.112	0.049	0.072	0.046	0.106	0.048	0.046

Table 2. Main physico-chemical parameters of lake waters in different years. *TDS – total dissolved solids, TDIC = (HCO_3^- + CO_3^{2-}), r – denotes equivalent concentration form throughout the table and further text

whereas calcium and potassium did not exceed 1.4 and 0.9 eq% respectively. As salinity increased in the lakes, there was a decrease in TDIC content and pH values, but other major anions and cations accumulated (Fig. 2). Some trace elements also concentrated accordingly. At maximum salinity levels we measured concentrations reaching: lithium – 1.5 mg/L, bromine – 369 mg/L, strontium – 18.5 mg/L, rubidium – 8.8 µg/L, selenium – 191 µg/L, uranium – 59 µg/L.

The ratios of rMg/rCa and rSr/rCa in the two lakes' waters changed differently. In Gorbunka Lake they grew along with increasing water salinity, whereas in Hilganta Lake such behavior persisted up to a salinity level of 41 g/L after which further increase in salinity led to reduction in those values.

Bottom sediments

A sediment core from Lake Gorbunka with a length of 30 cm was divided into layers of thickness 3–7 cm and additionally into 1-cm layers for studying the age of sediments. The stratigraphic sequence of individual sediment core layers is presented in Table 3. The sediment core from Lake Hilganta with a length of 38 cm was divided into layers of thickness 3–8 cm and additionally into 1-cm layers to study the age of sediments. The stratigraphic sequence of individual sediment core layers is shown in Table 4. According to X-ray diffraction data, the mineral fraction of sediments in the studied layers of both lakes contained universally at different mass concentrations: kaolinite, hydromica, quartz, feldspar, calcite, dolomite, halite, and traces of smectite, chlorite, and interstratified minerals. The ratio of mass fractions of lake bottom sediments minerals is represented in Figs. 3a, b.

Overall, in the lake sediments, the mass fraction of detrital material in the form of feldspar and quartz ranged from 60 to 92%. These minerals were found in large quantities in the sediments of Lake Hilganta (75–92%). In its sediment core section, their maximum amount was observed at a depth of 3–8 cm. Towards the bottom of the core, there was a decrease in their mass fraction with a small peak at depths of 18–23 cm. In the sediments of Lake Gorbunka, the content of quartz and feldspar varied between 55 and 72%. Their maximum quantity occurred within the layer 20–25 cm, while the minimum fell on the layer 4–7 cm. Carbonate minerals (calcite and dolomite) were detected throughout the entire cores of both lakes. In the sediment of Lake Gorbunka, calcite and dolomite most often existed in equal proportions (~5%) except for layers 7–12 and 20–25 cm where an

inverse trend in their accumulation was noted. In Lake Hilganta, traces of calcite were present in all sections of the core but increased up to 5% by weight at a depth of 18–23 cm. The mass fraction of dolomite was equal to 5% in upper sediment layers (0–8 cm) and in the interval 13–18 cm. Below these layers, dolomite was only traceable. Between calcite and dolomite in this lake's sediments, a mirror-symmetric distribution pattern of their mass fractions was more frequently observed. A similar distribution was also seen between the amounts of dolomite and clay (kaolinite + hydromica + smectites). An opposite dependence was also traced between the content of clay and feldspar. In the sediments of Lake Gorbunka such dependencies manifested themselves down to the layer 12–15 cm deeper towards the base clearly showing consistency in the distribution of mass fractions of calcite and clay as well as calcite and chlorite. In the sediments of Lake Hilganta these relationships were clearer except for chlorite which was not detectable across the whole thickness of its sediment or in the layer 23–30 cm where no clayey material was absent.

Bottom sediments of both lakes, with minor exceptions, contained halite, the mass fraction of which reached 20% in the layer 0–4 cm of Lake Gorbunka and 10% in the surface sediment layer of Lake Hilganta. It should be noted that at a depth of 3–8 cm in Lake Hilganta no halite was detected. In underlying layers it appeared only in trace amounts. In Lake Gorbunka, the decrease in the mass fraction of halite was observed down to the layer of 15–20 cm, but towards the bottom of the core its share increased.

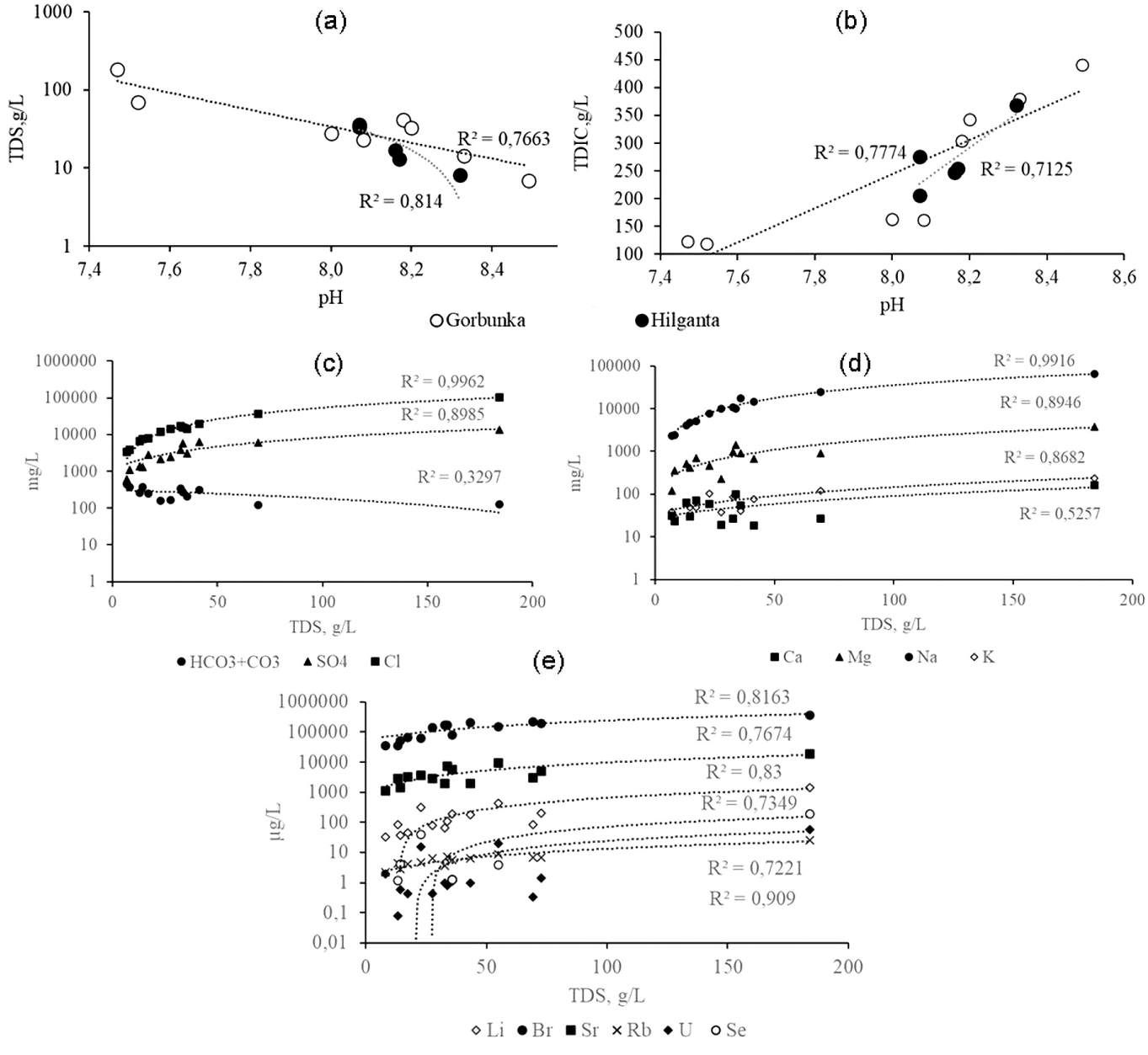

Fig. 2. Relationships between (a) pH and TDS, (b) pH and TDIC, (c) TDS with major anion concentrations, (d) TDS with major cation concentrations, and (e) TDS with some trace element concentrations

0-7 cm	7-12 cm	12-15 cm	15-20 cm	20-25 cm	25-30 cm
Wet, black clay with a sharp sulfurous smell and plant residues	Dense black clay with a sulfurous smell and plant residues	Dense gray clay with a faint sulfurous smell, without any plant remains	Dense grey clay with a faint sulfuric smell, containing plant residues	Dense grey clay with a slight clayey odor, containing a coarse fragment fraction with a diameter of 2-5 mm	Dense gray clay with a weak clayey odor, contains coarse-grained

Table 3. Physical and organoleptic data for individual layers of Lake Gorbunka sediment column

0-3 cm	3-8 cm	8-10 cm	10-12 cm	12-23 cm	23-30 cm	30-38 cm
Silt with a sharp sulfuric smell and plant residues	Dense gray clay with a faint earthy smell and a course-grained fraction	Dense grey clay with a faint clay odor	Dense gray clay with a faint clayey odor and a coarse fragment fraction	Soft gray clay with a faint clay scent and a coarse-grained fraction	Light-brown clay without any odor, with plant residues	Light brown clay without odor and with plant residues

Table 4. Physical and organoleptic data for individual layers of Lake Hilganta sediment column

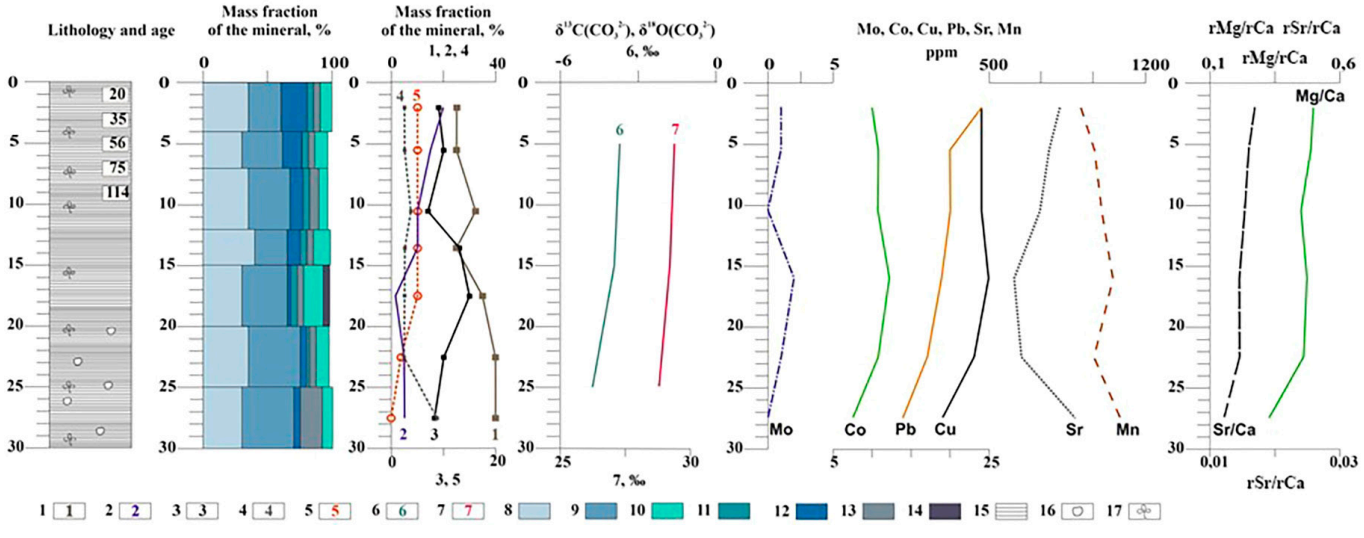

Fig. 3a. Lithologic column of Holocene section of Lake Gorbunka sediments, age model (^{210}Pb), distribution of mass mineral concentrations, carbonate $\delta^{13}C$ and $\delta^{18}O$ isotopes, bulk contents of Mo, Cu, Co, Pb, Mn and ratios rMg/rCa and rSr/rCa. 1, 9 – feldspars; 2, 12 – halite; 3, 10 – clay; 4, 13 – dolomite; 5, 11 – calcite; 14 – chlorite; 6 – carbon isotope ratio of carbonates; 7 – oxygen isotope ratio of carbonates; 15 – muds; 16 – coarse fragmental fraction; 17 – plant remains

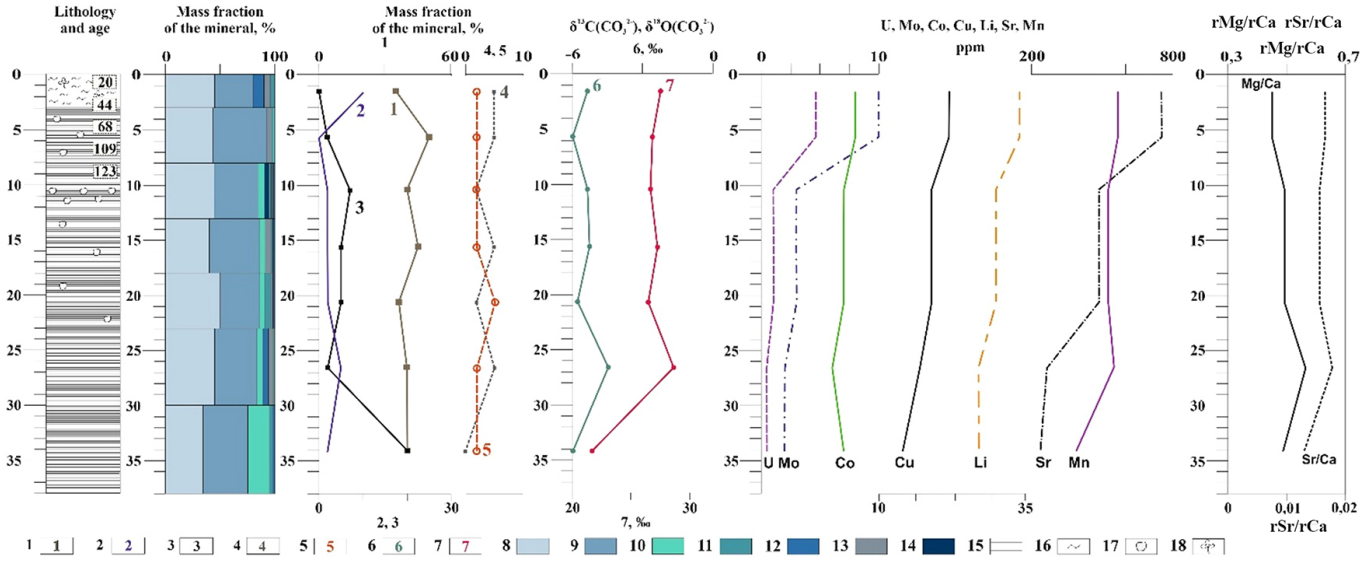

Fig. 3b. Lithologic column of Holocene section of Lake Hilganta sediments, age model (^{210}Pb), distribution of mass mineral concentrations, carbonate $\delta^{13}C$ and $\delta^{18}O$ isotopes, bulk contents of U, Li, Mo, Cu, Co, Sr, Mn and ratios rMg/rCa and rSr/rCa. 1, 9 – feldspars; 2, 12 – halite; 3, 10, 15 – clay; 4, 13 – dolomite; 5, 11 – calcite; 14 – amphibole; 6 – carbon isotope ratio of carbonates; 7 – oxygen isotope ratio of carbonates; 16 – muds; 17 – coarse fragmental fraction; 18 – plant remains

The distribution pattern for halite and ESP (presumably stands for another substance or parameter not specified here) most often showed an inverse relationship, except for the layers near the base of the cores where consistency in their quantity distribution was observed in both lakes.

In the gross fraction of chemical element content distribution determined by ICP-MS in the bottom sediments profile of Lake Hilganta, the highest bulk concentrations of Ca, Mg, Li, Sr, V, Fe, Zn, Sc, and Co occur in the layer from 0 to 8 cm, whereas those of Al, Ba, K, Na, Y – at the base of the core (Table 5).

In Lake Gorbunka, maximum concentrations for most elements were observed within the interval of 0–15 cm of the core. The previously noted significant excess concentration of Mg over Ca in lake waters diminished throughout the entire length of sediment cores. Furthermore, in the sediments of Lake Gorbunka, the ratios of rMg/rCa < 1. Along the entire core sections, the values of rSr/rCa in water and deposits are consistently below 1 and exhibit an uneven distribution. Minimal values of rMg/rCa and rSr/rCa were established at the bases of both lakes' cores.

To understand the complex behavior of chemical elements, their content was analyzed in sediment cores from Lake Hilganta using various extracts, taking into account their total concentrations in individual layers. The highest amount of Na was found in the layer 0–8 cm at stage "A" corresponding to dissolution of water-soluble fraction of sediments (salts). Throughout the core length there was a direct relationship between Na content and feldspar quantity. At leaching stage "B", Ca, Mg, Sr, Ba, B, Mn, REE, B, Y and U were concentrated in large amounts (Table 6); these elements are part of carbonates, oxides and hydroxides (Borzenko, 2020).

Overall, there was consistency in the distribution of the listed elements' quantities in this solution with respect to the amount of dolomite or calcite across the core section from the upper layer to the base.

Maximum contents of Li and Al were identified in the layer 0–8 cm, while P, K, Fe, Ni, Se, Zr, Th, Nb, As, Zr, Nb, REE, Pb, Cu, Zn, As were found at their highest levels in the layer 23–30 cm during stage "D" corresponding to the decomposition of aluminosilicate and silicate fractions. In this case, the curves representing element content distributions along the entire length of the core completely mirrored the curve for mass fraction of feldspar. Silicon is concentrated in maximum amounts within the layer 23–30 cm at the organic matter decomposition stage ("C").

Parameters	Gorbunka						Hilganta						
cm	0-4	4-7	7-12	12-15	15-20	20-25	0-3	3-8	8-13	13-18	18-23	23-30	30-38
Al	5.69	6.2	6.34	6.7	6.05	5.43	54000	62300	60000	61000	60100	62700	65500
Ba	452	499	506	529	501	481	365	502	507	563	542	540	589
Ca	45400	45800	45100	40900	43000	68100	6100	4660	3850	3820	3410	2960	3390
Co	10	11	11	12	10	7	10	9	8	8	7	7	7
Cu	24	24	24	25	23	19	33	28	34	23	20	19	18
Fe	27500	29200	29800	29700	27100	20000	29000	27000	24800	25000	22600	22900	24000
K	19800	21400	21600	23600	21400	21000	17600	21900	22900	24800	23600	23400	25400
Li	49	52	51	50	45	31	43	38	33	32	28	28	30
Mg	23000	22300	20700	19400	19800	22600	24800	19200	18700	18800	16800	11500	9500
Mn	855	915	936	979	912	1010	709	735	725	746	659	483	412
Mo	1	1	<1	2	1	<1	11	3	2	2	2	2	3
Na	43100	35000	27500	26900	25700	22900	21500	19700	21200	22100	22300	23600	22800
P	600	600	600	600	600	500	900	600	600	600	500	400	400
Pb	24	20	20	19	17	14	18	17	16	17	18	16	18
Sc	8.6	9.2	9.4	9.8	8.6	6.4	7.5	7.5	6.9	6.8	6.4	6.7	7.2
Sr	770	736	692	596	628	838	1010	695	622	614	547	372	334
V	65	71	72	76	64	41	76	66	54	53	50	54	59
Y	16.5	17	18.1	17.9	16.8	14.2	15.4	16.4	15.7	15.9	15.2	16.4	17.4
Zn	72	71	72	73	67	50	63	59	54	53	49	48	49
Zr	75.6	74	80.8	75.9	70.6	60.4	60.4	62.9	58.4	61.4	57.1	63	62.7
S	5300	4600	3400	3000	2700	1400	8000	2900	3700	3000	2700	2300	2600
Si	900	1200	1500	1300	1400	1100	1400	800	1000	800	400	400	400
rMg/rCa	0.84	0.81	0.76	0.79	0.77	0.55	6.78	6.87	8.10	8.20	8.21	6.48	4.67
rSr/rCa	0.170	0.161	0.153	0.146	0.146	0.123	0.166	0.149	0.162	0.161	0.16	0.126	0.099

Table 5. Concentrations of chemical elements (ppm) and values of rMg/rCa and rSr/rCa in separate sediment layers of two lakes

Parameters	Stage A				Stage B			Stage C			Stage D		
	0-8	8-23	23-30	30-38	0-8	8-23	23-30	0-8	8-23	23-30	0-8	8-23	23-30
Li	0.71	<по	<по	<по	5.73	4.61	3.59	8.41	5.60	3.42	9.30	5.06	8.51
B	12.72	6.11	3.61	3.83	31.66	15.32	5.96	3.21	3.05	1.08	9.17	4.83	4.98
Na	4346	2873	3205	3048	256	212	122	56	36	84	<по	211	1033
Mg	1796	1281	1174	1131	14930	7694	2172	2336	1675	394	2339	1223	2452
Al	0.4	4.5	6.0	3.8	993.6	736.2	675.9	3585.9	2490.4	1595.9	13078.1	7453.8	10141.4
Si	28.0	14.0	21.6	93.1	633.9	539.7	469.0	649.4	529.1	702.8	56.7	56.5	182.8
P	<по	17.9	<по	15.3	180.7	142.3	71.1	100.8	83.4	28.8	298.6	212.8	345.0
S	<по	<по	<по	<по	58	30	32	<по	<по	<по	<по	<по	<по
K	<по	<по	<по	<по	358	489	426	678	528	245	1138	693	1396
Ca	349	418	396	504	9015	4490	1135	457	349	141	294	287	1331
Fe	9.6	20.0	<по	23.3	2080.0	1478.0	1057.3	3674.0	2953.5	1657.6	6351.6	3729.7	6891.3
Mn	0.7	0.8	0.8	0.3	468.6	362.3	123.1	76.0	49.3	40.5	85.1	55.8	113.2
Co	<по	0.12	0.11	<по	3.94	3.25	3.06	4.64	2.54	1.39	3.46	2.09	3.89
Ni	1.29	1.44	1.02	1.51	18.89	12.47	11.36	8.61	6.69	1.96	26.00	22.48	29.75
Cu	1.53	<по	<по	0.69	0.51	1.86	2.14	13.52	8.94	2.79	14.93	26.05	76.60
Zn	1.35	1.73	2.23	2.19	3.79	7.45	0.10	16.27	12.03	7.91	23.03	144.14	429.14
As	<по	0.36	0.11	0.20	1.25	2.05	1.06	2.00	1.55	0.93	8.84	7.80	18.64
Se	0.42	<по	<по	0.27	0.27	0.34	2.10	<по	0.43	<по	12.73	7.65	24.34
Rb	64.7	69.9	74.6	21.3	1.1	1.2	0.8	7.4	5.5	3.5	21.8	11.9	21.2
Y	<по	<по	<по	<по	5.57	4.49	3.90	4.33	2.60	1.20	2.43	1.60	2.89
Zr	0.05	<по	0.05	0.03	0.89	0.39	0.59	0.08	0.08	<по	12.40	8.66	14.58
Nb	0.00	<по	0.00	0.00	0.02	0.01	0.01	0.01	<по	0.14	0.81	0.45	1.73
Mo	9.15	4.18	4.65	10.44	0.71	0.34	0.13	<по	<по	<по	1.88	0.59	1.28
Ba	9.7	10.8	12.5	26.1	61.2	51.6	48.0	53.1	37.5	7.7	33.9	16.3	29.1
REE	0.17	0.06	0.07	0.06	37.46	31.10	27.75	36.65	23.84	11.88	33.54	21.14	39.07
Pb	0.60	0.70	0.59	0.84	0.62	0.29	0.16	4.05	3.19	1.91	4.91	5.97	17.12
Th	<по	<по	<по	<по	33.78	5.91	2.20	2.41	1.73	1.00	4.42	2.76	6.33
U	4.09	0.71	0.15	0.16	4.66	1.05	0.50	0.90	0.97	0.12	0.74	0.46	0.64

Table 6. Chemical element content (ppm) in different leaching stages for individual bottom sediment layers of Lake Hilganta

Age and sedimentation rate

Knowing the dates of the most significant radionuclide releases into Earth's atmosphere makes it possible to determine the age of bottom sediments and calculate sedimentation rates based on their depth in deposits. For example, large-scale nuclear weapons testing began in 1958. However, maximum intensity was reached at the beginning of the 1960s, which is often recorded in vertical distribution profiles of radionuclides in cores from different regions worldwide. From that year onwards, land-based and airborne explosions gradually ceased, leading to a sharp decline in radionuclide concentrations within bottom sediments. In Lake Hilganta, specific activity of atmospheric $^{210}P_{atm}$ decreased down to minimal values at a depth of 12 cm (Fig. 4); thus, the calculated lower boundary for the determinable period corresponds to 1899 AD. In Lake Gorbunka, minimum value of "excess" $^{210}P_{atm}$ was determined in a layer at 27 cm depth dated back to 1907 AD.

According to estimates derived from vertical distributions of excess $^{210}P_{atm}$ activities in Lake Hilganta, average sediment accumulation rate during formation of 12-cm-thick bottom sediments amounts to 0.8 mm per year. Sedimentation rate in Lake Gorbunka is twice as high compared to Lake Hilganta.

Isotopic ratios of $^{18/16}O$ and $^{13/12}C$ carbonates

Relatively high values of $\delta^{18}O$ in the surface layers of two lakes and also at a depth of 23–30 cm in Lake Hilganta may indicate higher salinity of waters during carbonate formation. Conversely, lower $\delta^{18}O$ values suggest an increase in water content of the lake basin due to dilution by freshened water. Changes in $\delta^{13}C$ values of carbonates throughout sediment thickness occur as a result of extraction of ^{12}C through photosynthesis when primary biological productivity increases during dry periods, and input into the lake of soil-derived CO_2 enriched with lighter carbon isotope (–12‰) during wetter conditions on the territory (Galimov, 1968).

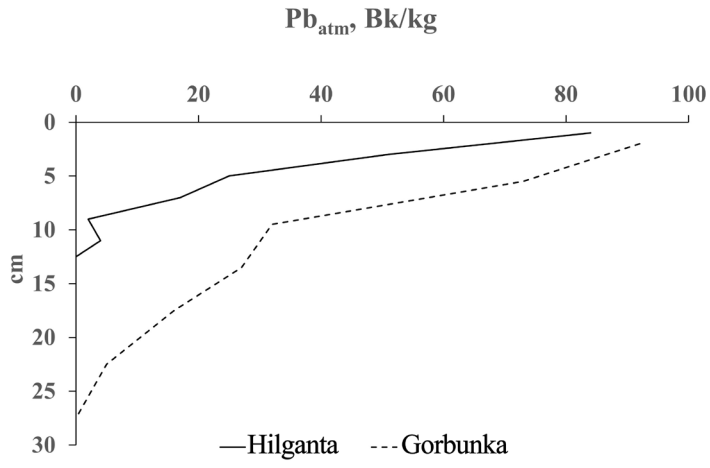

Fig. 4. Vertical profiles of ^{210}Pb activity in lake bottom deposits

Discussion

Factors controlling the chemical evolution of lakes

The climatic factor

Based on the actual data obtained from isotopic, mineralogical and chemical compositions of sediments in two lakes, areas of sedimentation have been identified corresponding to stages of "shallow" and "deep" lakes. According to dating results (based on ^{210}Pb activity), the most significant changes in water level and transition between these states occurred over the last 20-25 years. This period has already been mentioned as a transitional one from wet to dry conditions (Obyazov, 2007). The possibility of reduced water volume during the period of 2014–1999 due to climate aridization was confirmed by a decrease in the proportion of coarse-grained material and consequently lower mass fraction of terrigenous feldspar and quartz in the surface layer of bottom sediments in both studied lakes. During this time interval, halite content reached its maximum values. Simultaneously, there were maxima in Sr/Ca ratios, metal and metalloid contents, as well as heavy oxygen and carbon isotopes in carbonates.

Apparently, a "deep" lake existed during the periods of 1986–1978, 1913–1907 and in 1899. These events were accompanied by the presence of clastic material in corresponding layers of the lake, an increase in mass fraction of calcite and dolomite, as well as a decrease in halite and clay fractions. Carbonates were isotopically lighter everywhere in terms of carbon and oxygen. The values of rSr/rCa were also relatively low. Consistency in dates of lake filling was traced according to hydrological data obtained from observations on the largest lakes in this region – Barun-Torey and Zun-Torey, which were abundant with water during these periods (Zamana, Obyazov, 2004). According to the same authors, Toreyskie Lakes dried up in the mid-1940s. In sediment layers corresponding to that period, there was no clastic material present, the amount of calcite and dolomite decreased while the amounts of clay and halite increased. Additionally, in the sediments of Lake Hilganta, the values of δ^{13}C and δ^{18}O for carbonates rose.

Deeper into the core section (undated layers), an uneven distribution of mass ratios of calcite, dolomite, PS, clays and halite was observed in combination with the amount of chemical elements in the bulk fraction and corresponding leachates. The isotopic ratios of oxygen and carbon in carbonates changed sympathetically. A particularly distinct layer at a depth of 23–30 cm from Hilganta Lake core (~ mid-18th century calculated based on average sedimentation rate) was noted earlier for a sharp increase in halite mass ratio, accumulation of some chemical elements and heavy isotopes of carbon and oxygen in carbonates, increased values of rMg/rCa and rSr/rCa, as well as absence of coarse detrital material fraction. Such distribution of all considered components indicates a decrease in lake water volume due to changes in territory humidity.

It is evident that variations in water level resulting from fluctuations in climatic parameters were reflected in processes of interaction between water and host rocks. Since many minerals are not stable and can easily precipitate or dissolve depending on temperature oscillations, salinity, pH of water, and biogeochemical processes.

Water rock interaction

Transformations in the chemical composition of bottom sediments are a result of changes in thermodynamic equilibria in the system "water – rock", which can be theoretically calculated using programs for physico-chemical modeling applicable to multicomponent systems. The latter include minerals that come into contact with water and the water itself, having different ionic compositions. An equilibrium state was considered for a system formed by 19 chemical elements (H, C, O, S, Cl, Na, Ca, Mg, Si, K, Fe, Mn, Al, F, P, Sr, Pb, Mn, Zn), 100 simple and complex particles, and 50 potential minerals (metal hydroxides, carbonates,

sulfates, chlorides, quartz, kaolinite, montmorillonites, illites, micas, plagioclases, feldspars, etc.).

Considering that groundwater is the main source of chemical elements in lakes, it was primarily necessary to understand the processes occurring in the system "groundwater-rock". The possibility of forming authigenic aluminosilicate minerals, particularly clays, is dictated by the following conditions. Saturation of water with kaolinite $Al_2Si_2O_5(OH)_4$ can occur already at TDS = 0.1 g/L, pH = 6.9, Si content = 0.37 mg/L and Al = 0.18 μg/L. For montmorillonite formation $Al_2Si_4O_{10}(OH)_2$ and illites $K_{.56}Na_{.04}Mg_{.24}Al_{2.68}Si_{3.22}O_{10}(OH)_2$, salinity must be over 0.2 g/L, pH > 7.1–7.5, and Si content > 4.5 mg/L (Borzenko, 2020). To form calcite $CaCO_3$, water salinity should exceed 0.6 g/L and pH > 7.3. A slight increase in water salinity (> 1.0 g/L), pH, and concentrations of Ca^{2+} + Mg^{2+} (> 0.01 g/L) leads to saturation with dolomite $CaMg(CO_3)_2$. At the same time, all groundwaters remain out of equilibrium with such sulfate minerals as gypsum $CaSO_4(H_2O)_2$, bledite $Na_2SO_4 \cdot MgSO_4 \cdot 4H_2O$, glauberite $Na_2SO_4 \cdot CaSO_4$, mirabilite $Na_2SO_4(H_2O)_{10}$ etc. Groundwaters are also not in equilibrium with hydrohalite $NaCl \cdot 2H_2O$ and halite NaCl. No equilibrium is observed concerning the most common minerals found on lake shores, such as plagioclase (mainly $NaAlSi_3O_8$), quartz (SiO_2), pyroxenes ($Me_2^{2+}[Si_2O_6]$), which were detected in the coastal zone of lakes. Therefore, during high-water periods these minerals may enter lacustrine sediments from watersheds and serve as sources of many chemical elements and secondary mineral formations.

For thermodynamic calculations of equilibria in the system "lake water – rock", measured physico-chemical parameters of lake water were entered into the database. Evaporation and subglacial concentration were carried out by removing H_2O until a salinity of 360–380 g/L at temperatures of 0 and 22 °C was reached. Naturally, during winter the temperature of highly saline water could be negative, but this fact was not taken into account due to limitations of Pitzer's database.

According to modeling results, the chemical type of lakes did not change with decreasing volume of water. The initial solution with a salinity of 7–8 g/L (Na-Cl chemical type) was already in equilibrium state relative to illite, smectite, and kaolinite (Fig. 5).

A relatively high value of saturation degree lgQ/K for clays was observed at 0 °C. Moreover, as the salinity increased, the value of lgQ/K also increased. Equilibrium between waters and primary host minerals such as plagioclase, pyroxene, and quartz was not achieved.

Saturation of waters relative to strontianite SrCO3 was observed exclusively in Lake Hilganta up to a salinity of 40 g/L and pH = 8.5 (at 0 °C). At both temperatures, dolomite saturation occurred throughout the entire range of salinities in Lake Hilganta. In Lake Gorbunka, as salinity increased, the water saturation index with respect to dolomite gradually decreased, becoming equilibrated at 0 °C and pH < 8.1 for salinities > 70 g/L. For calcite, the highest value of log Q/K was noted at T = 22 °C in both lakes up to a salinity of approximately 17 g/L and pH values between 8.17 and

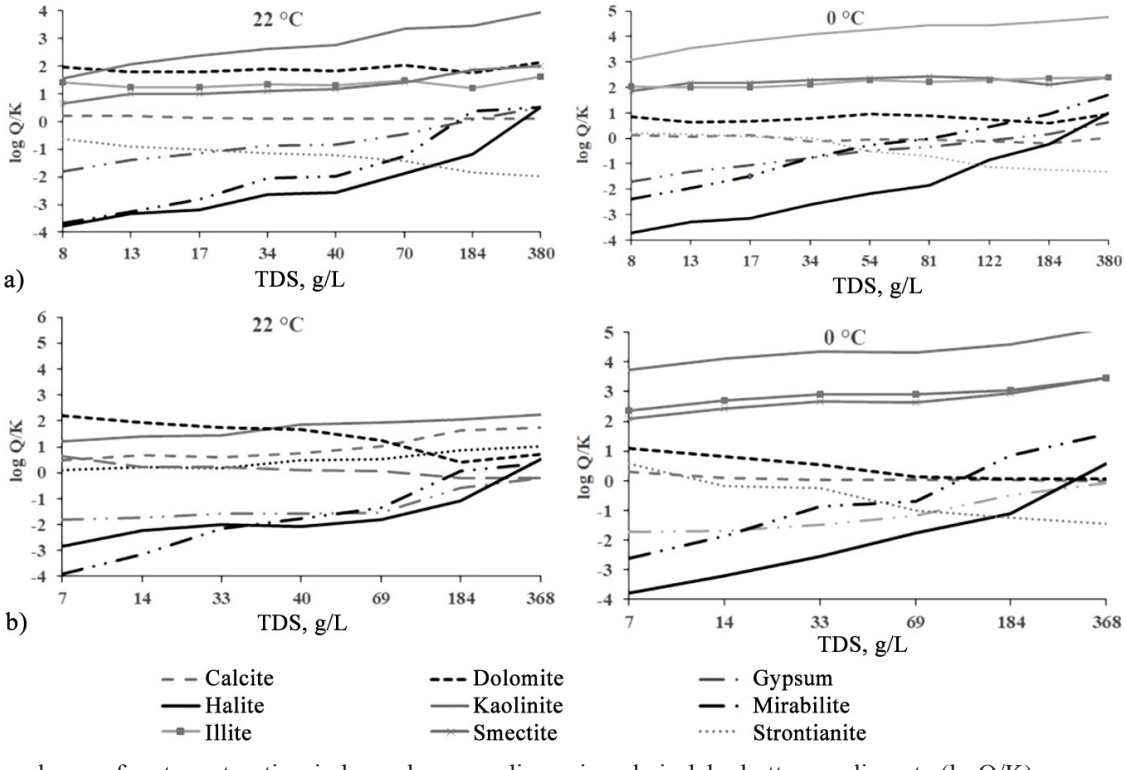

Fig. 5. Dependence of water saturation index value regarding minerals in lake bottom sediments (lg Q/K) versus salinity and temperature of water (a) Hilganta and (b) Gorbunka

8.25. Above this established salinity level, lake waters were found to be in equilibrium with calcite at 0 °C.

It has been noted that the decrease in lgQ/K values for calcite and dolomite coincided with an increase in lgQ/K values for gypsum and mirabilite. Thermodynamic equilibrium of water with gypsum was only established for Lake Hilganta at a water salinity of 184 g/L and pH 7.2. Bąbel & Schreiber (2014) emphasized that the process of gypsum crystallization may depend on the amount of halite present. Saturation of waters with halite NaCl was observed at salinities greater than 368 g/L. According to calculations, water equilibrium with mirabilite is possible at 0°C when total dissolved solids (TDS) are > 80 g/L, and at 22 °C when TDS > 184 g/L in both lakes. However, X-ray diffraction analysis did not detect sulfate minerals in sediments. The lake waters also proved non-equilibrium with soda minerals such as gaylussite, nahcolite, soda etc.

Biogeochemical factor

It is known that the solubility of $CaSO_4 \cdot 2H_2O$ increases significantly with increasing concentration of NaCl in solution, therefore sodium chloride brines have a huge capacity to accumulate SO_4^{2-}. The processes of gypsum and mirabilite formation were not established in bottom sediments, probably due to well-known interdependencies between the processes of gypsum and carbonate mineral formation since "the conditions for gypsum formation exclude those for carbonates and vice versa" (Lange, Krijgsman, 2010). According to our previous studies (Borzenko, Shvarsev, 2019; Borzenko, Fedorov, 2024), hydrogen sulfide formed as a result of bacterial sulfate reduction processes is present almost everywhere in the bottom water layer and bottom deposits of saline lakes in Transbaikalia, so sulfur in bottom sediments mainly exists in reduced form (Borzenko, 2020). It is evident that dolomite formation process can proceed synchronously with bacterial sulfate reduction according to the reaction:

$CaCO_3 + Mg^{2+} + C_{opr} + SO_4^{2-} + 2H^+ = CaMg(CO_3)_2 + HS^- + OH^-$.

This reaction explains the frequently observed mirror-symmetric distribution of calcite and dolomite mass fractions along the core section. Moreover, according to Sonnenfeld (1988), dolomite becomes more stable at pH above 7.8 (while calcite stabilizes at pH above 7.4). Apparently for this reason its relatively high contents in sediments were recorded during the period of a "deep" lake against the background of water freshening and increasing pH.

It turns out that this process controls, on one hand, the formation of dolomite in the anaerobic zone, while on the other hand, upon oxygen influx from the oxidative zone – calcite. Of course, both calcite and dolomite can form under either anaerobic or aerobic conditions (Kolpakova et al., 2019), which explains their synchronous distribution within individual sediment layers.

The main mechanisms of lake evolution

To reconstruct in detail the mechanisms occurring during transformation of saline lake deposits, it is necessary to understand all interaction processes within the "water–rock" system. As known, aluminosilicates dissolve via hydrolysis mechanism (Keller, 1963). Based on alumino- and silicate hydrolysis reactions, OH^- appears in water equivalent in quantity to positively charged cations (Me^{n+}); however, under real natural conditions dissolved CO_2 always exists in water, which reacts with OH^- forming HCO_3^- (Shartsev, 2000). Thus, two opposing processes occur simultaneously in this system: according to W.D. Keller's reaction pH increases while following Shvartsev's reaction it decreases. If we add that simple evaporation under laboratory conditions, i.e., when there is no interaction between water and rocks, leads to a decrease in solution pH (McCaffrey et al., 1987), then it becomes clear why increasing water salinity causes a reduction in pH.

As shown above, the groundwater feeding lakes is not only saturated with respect to kaolinite and illite but also includes montmorillonites of various compositions (Mt-Ca, Mt-Na, Mt-K). At the same time, these waters remain out of equilibrium with many other aluminum silicate minerals from lake catchments, meaning they will continue interacting with water and serve as a source of chemical elements (Garrels, Christ, 1965; Shartsev, 1991; Nordstrom et al., 1989 etc.). Once entering lakes, this water finds itself in conditions where its evaporation rate increases, leading not only to concentration of Cl^- and SO_4^{2-} ions but also of other elements including Na, Mg, etc. Our studies demonstrate that processes occurring within lakes involve not just water evaporation but continued interaction with rocks. Therefore, clay minerals continue forming. While some fraction undoubtedly comes from the catchment area, an increase in their mass proportion along with simultaneous decrease in plagioclase content during dry periods proves the possibility of their formation directly within lakes themselves. Furthermore, evidence supporting the fact that plagioclases are sources for numerous chemical elements (including Na) lies in the concordant distribution pattern between most element contents and their total mass presence across sediment layers.

However, despite the presence of geochemical barriers in the form of secondary minerals, many chemical elements accumulate in lake water with increasing salinity. Relatively high concentrations of Ca, Mg and Sr are observed in lake water at its maximum salinity and minimum pH. Thermodynamic calculations have shown that saturation degree relative to carbonate minerals decreases as water salinity increases. Thus,

when salinity reaches 40 g/L, waters become non-equilibrium with respect to strontianite, so under higher salinity but lower pH conditions, strontium begins to accumulate in water. From this point on, the values of rSr/rCa change significantly.

With regard to calcite and dolomite, waters are supersaturated relative to dolomite up to a salinity of approximately 70 g/L, and relative to calcite up to a salinity of about 17 g/L. Considering that the ratio rMg/rCa in waters varies from 6 to 61, according to Drever (2005), besides dolomite, magnesium calcites, aragonite, magnesite and other Mg-minerals should also be formed in sediments. However, apart from these mentioned carbonate minerals, no other forms were detected. This is explained by changes in migration forms of Mg and Ca with increasing water salinity. If underground waters and during desalination periods of lake waters dominate Me^{2+} and $MeCO_{3(aq)}$, whose contents are controlled by carbonates (Borzenko et al., 2021), then in lakes at a salinity of ~40 g/L, dominant forms already include $MeSO_{4(aq)}$ and $MeCl^{+}$ (Fig. 6).

Further increase in salinity is accompanied by the accumulation of exclusively $MeCl^{+}$. At the same time, the proportion of carbonate complexes remains relatively low (< 1 mol%).

It is likely that in these lakes water evaporates faster than OH^{-} and consequently HCO_3^{-} are concentrated, so salinity and concentrations of mobile elements (Na, Ca, Mg, Li, Br, Sr, Rb, Se and U) grow. In sediments heavy isotopes of oxygen and carbon from carbonates accumulate while the amount of TDIC (TDIC = HCO_3^{-} + CO_3^{2-}) and pH of waters decrease. If the amount of TDIC does not increase in a lake then contents of Cl^{-} and SO_4^{2-} become higher forming chloride or sulfate types of lakes.

The simplest method for predicting the direction of lake evolution is using the "Spencer triangle" (Fig. 7a).

The Ca–SO_4–(CO_3 + HCO_3) system can be illustrated on a ternary phase diagram. The content of these components can be plotted on this diagram using equivalent concentrations of Ca, TDIC and SO_4 in waters. It is known that at the initial stage of evaporative concentration of water accompanied by calcite precipitation leads to changes in the chemical composition of water towards the boundary between TDIC and SO_4 (Hardie, Eugster, 1970), as shown by arrows in Fig. 7a. Waters with composition 1 precipitate sodium carbonates at the final stage of evaporation, while waters with composition 2 precipitate sodium sulfate. All waters may at some point precipitate halite (for more details see Spencer, Hardie 1990). Transition from calcite to gypsum represents the boundary between "Neutral" and "Calcium Chloride Acidic" waters. Neutral waters such as composition 3 precipitate calcite and are removed directly from the calcite composition. Continued concentration and precipitation of calcite lead into the stability region of gypsum. Waters along this boundary are depleted in TDIC, and gypsum is the predominant precipitate.

Further concentration is accompanied by precipitation of halite and many other salts including potassium and magnesium sulfates and chlorides. Calcium-chloride waters like composition 4 precipitate calcite and are removed directly from the calcite composition. Further evaporative concentration and calcite precipitation bring these waters into the stability area of gypsum located along the boundary between Ca and SO_4. Waters move along the phase boundary from the gypsum composition point toward the Ca corner of the diagram. These waters are depleted in SO_4, and further concentration results in precipitation of halite as well as potassium, magnesium and calcium chlorides.

The relationship between Mg and Ca can be investigated using the Spencer triangle by replacing the vertex of Ca with Mg (Fig. 7b). For groundwater, the ratios of three components are located in the lower right corner of the triangle, then water will evolve

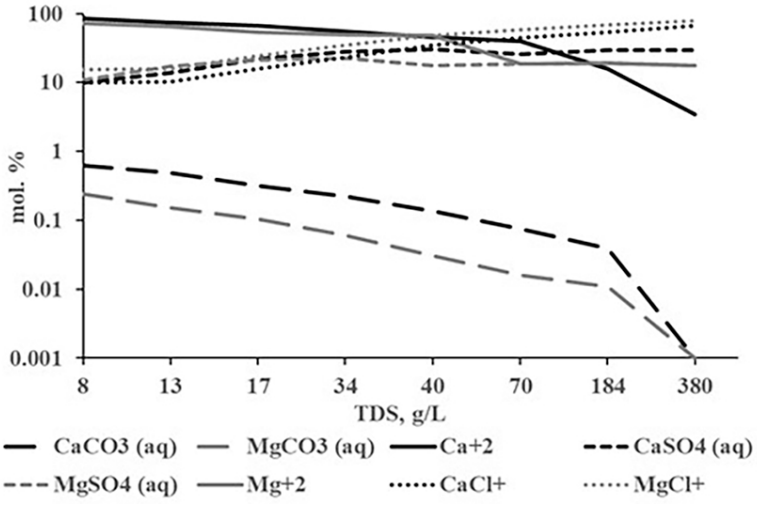

Fig. 6. Major migration forms of Ca and Mg in lake waters

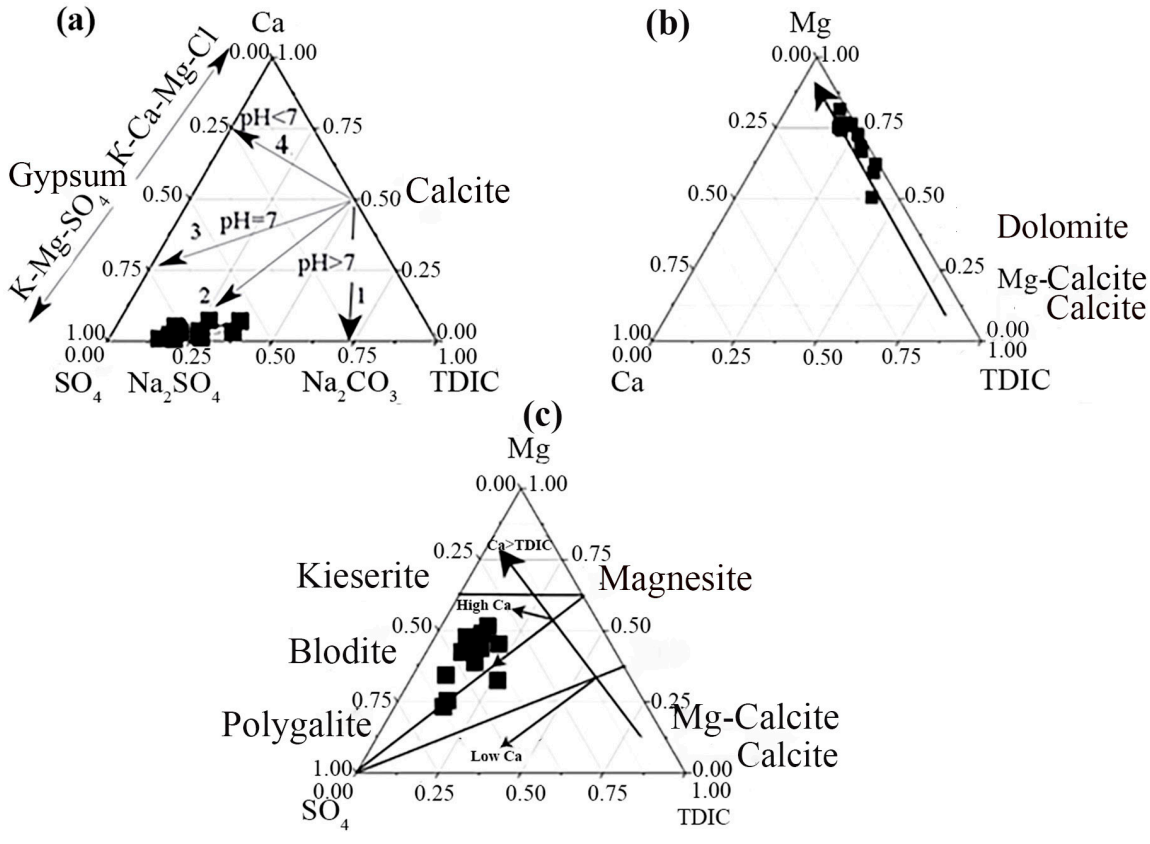

Fig. 7. Ternary phase diagrams in systems: a) Spencer triangle, Ca–SO_4–HCO_3 b) Mg–TDIC–Ca and c) Mg–TDIC–SO_4 illustrating composition during evaporation process of Lakes Hilganta and Gorbunka waters

towards the upper left corner (Fig. 7b), moving away from calcite or Mg-calcite point. Four arrows on the triangle (Deocampo, Jones, 2014) (Fig. 7c) represent four conditions with different rCa/rMg ratios that form Ca-Mg carbonates and Mg-carbonates at various times. Waters low in calcium content produce Mg-bearing carbonates earlier than waters high in calcium. Predicting the exact timing of this process is difficult because it depends on poorly understood kinetic processes. It also depends on Mg binding to authigenic clay minerals which may significantly affect Mg concentration (Borzenko, Shvartsev, 2019). Once Ca has been depleted and sufficient amount of produced TDIC allows dolomite formation, points characterizing water composition shift toward the apex of Mg-TDIC axis, thus determining molar ratios rMg/rSO_4 and rSO_4/rTDIC in residual fluid.

Müller and Teitz (1971) studied the formation and diagenesis of inorganic Ca-Mg carbonates in 25 lakes across Europe, the Middle East, and Africa. The salinity of these brines was over 400 g/l (for example, Lake Tuz). Precipitation of Mg-calcite occurred with solutions having an rMg/rCa ratio from 2 to 7. When this ratio exceeded 12, aragonite precipitated. An rMg/rCa ratio > 7 in water leads to dolomite formation, while a ratio > 40 transforms dolomite into huntite or magnesite. Interactions between Ca-Mg carbonates and aqueous rCa/rMg ratios are particularly well illustrated by sediment core during relatively rapid lake level decline at the end of the last glacial period in Lake Bonneville (Jones et al., 2009). In this interval of the core, the proportion of carbonate mineral steadily increases accompanied by increasing Mg content in calcite up to 11 mol %, after which aragonite becomes the dominant carbonate phase. Dolomite then also appears in the sediment column. The Mg and silica content of the clay fraction gradually increase due to kerolite (hydrated talc) interstratification within detrital smectite (Jones, Spencer, 1999). Authors conclude that formation of these two phases will depend on relative excess of aquatic silica and alkalinity of the system rather than just magnesium concentration. In highly alkaline lakes of Eastern Africa, clayey Mg minerals precipitate earlier than carbonates from relatively dilute waters (Deocampo et al., 2009, 2010).

It turns out that, firstly, the process of interaction between water and aluminosilicate rock does not allow the pH value of water to shift into the area of "acidic" waters as a result of their evaporative concentration, since OH^- appears in the water, and secondly, due to sulfate reduction, calcite transforms into dolomite, accumulates OH^-, and consequently increases the pH of water.

A schematic representation of the general chemical composition of water formed as a result of these factors, with increasing relative solubility from top to bottom, is presented in Fig. 8.

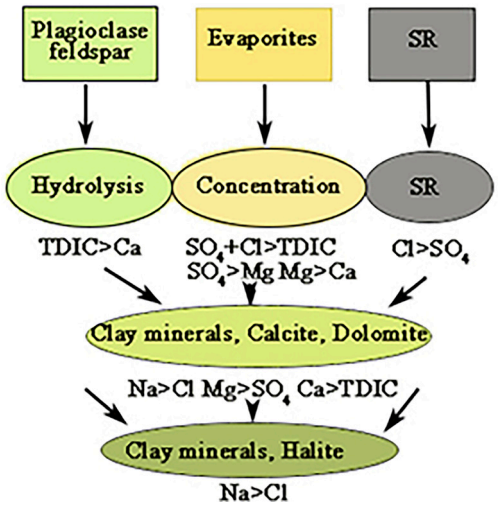

Fig. 8. Block diagram depicting evolution of water highlighting specific conditions for studied lakes. Primary processes are framed, dissolved components marked outside frames, while mineral precipitates and their formation mechanisms indicated by oval shapes. SR stands for sulfate reduction

In the diagram, dissolved substances (Ca, Mg, Na, TDIC, SO_4, Cl) are referred to total amount of aqueous compounds in equivalents. The scheme shows that conditions Ca > TDIC favoring gypsum precipitation occur at one of the last stages of lake evolution (TDS = 184 g/l and pH < 7.2). On the other hand, condition TDIC > Ca occurs in more alkaline solution. At the same time, everywhere the amount of Mg is significantly greater than TDIC. Clay formation resulting from hydrolysis of aluminosilicates and silicates takes place over the entire range of salinity, so they will be present in sediments and limit step by step mobility in waters not only some part of Ca, Mg, Na, K, Si, Al but also many trace elements (Shvartsev, 2000), including through sorption processes (Pechenyuk, Semushina, 2021). Bacterial sulfate reduction will change the ratio of Cl and SO_4. Dolomite formation will alter the relationship between Na and Mg. The role of TDIC will gradually decrease under dominant evaporation process, therefore the pH of the solution will gradually decrease. Appearance of halite should lead to balancing Na with Cl, but ongoing hydrolysis process will provide additional portion of Na. Since initial solution represents Cl Na type, it will remain such throughout the considered period.

Conclusion

The article presents detailed hydrogeochemical studies of bottom sediments in the chloride lakes Gorbunka and Hilganta. The lakes are located in a semi-arid climate and represent the most rare for this region Cl-Na chemical type. They are endorheic with unstable hydrological regimes. During dry periods they become shallower, while during wet periods their water volume increases. Aquatic environment has neutral pH at higher salinity levels but becomes alkaline when salinity decreases. With increasing salinity there is no accumulation of TDIC in water, but Cl^- and SO_4^{2-} ions concentrate instead, however the increase in Cl^- content outpaces that of SO_4^{2-}. Simultaneously, elements such as Na, Ca, Mg, Li, Br, Sr etc., accumulate synchronously.

Based on the activity values of "excess" ^{210}Pb, ages of individual layers of bottom sedimentation and rates of sedimentation were determined. These data correlate well with previously noted dates of drying up and filling of the largest regional lakes Zun and Barun Torey. Together with data on ^{210}Pb and distribution of mineral contents across the depth profile of bottom sediments, two stages of sediment formation have been established: the stage of "shallow" lake and the stage of "deep" lake. The more "shallow" period is represented by deposits of minerals like halite, calcite, dolomite, clays. In contrast, the more "deep" period (after abrupt changes in the lake's water balance), mineral complexes are characterized either by absence or trace amounts of halite, larger portions of dolomite and feldspars.

The data on chemical element fractionation along the core also indicate changes in geochemical balance during these two periods. High proportions of water-soluble fractions of Na, as well as carbonate Ca, Mg, Fe, oxide and hydroxide Fe, Mn, U, REE and others during high salinity waters due to their intensive evaporation determine differences between "shallow" and "deep" stages of lakes.

Thermodynamic calculations have shown that newly formed minerals limit the contents of many chemical elements preventing them from accumulating in aqueous solution. Such selective concentration leads to deep differentiation of chemical element ratios in bottom sediments.

Bacterial reduction of sulfate ions limits its content in waters, therefore Cl^- accumulates in large quantities. Moreover, under hydrogen sulfide conditions dolomite formation becomes preferable while under oxygenated conditions calcite is favored.

Changes in lake geochemical balance resulting from climatic fluctuations are mainly caused by changes in the "water-rocks" system and evaporation processes combined with intermittently active biogeochemical processes.

Acknowledgements

The work was supported by the Fundamental Research Program of the Siberian Branch of the Russian Academy of Sciences.

References

Bąbel M., Schreiber B.C. (2014). Geochemistry of Evaporites and Evolution of Seawater. *Treatise on Geochemistry*: Second Edition, Vol. 9. doi: 10.1016/B978-0-08-095975-7.00718-X

Bazarova V.B., Grebennikova T.A., Mokhova L.M., Orlova L.A. (2011). Holocene lake sedimentation in the steppe zone of Southeastern Transbaikalia (exemplified by the sediments of lake Zun-Soktui). *Russian Geology and Geophysics*, 52(3), pp. 333–342. https://doi.org/10.1016/j.rgg.2011.02.006

Bezrukova E.V., Amosova A.A., Chubarov V.M., Finkelshtein A.L., Kulagina N.V. (2017). Environmental changes in the northeast of the Buryat republic during the holocene post-optimum: first results. *Contemporary Problems of Ecology*, 10(4), pp. 431–440. (In Russ.) DOI: 10.15372/SEJ20170410

Boros E., Horváth Z., Wolfram G., Vörös L. (2014). Salinity and ionic composition of the shallow astatic soda pans in the Carpathian Basin. Ann. De Limnol. *Int. J. Limnol.*, 50, pp. 59–69. doi: 10.1051/limn/2013068

Borzenko, S.V. (2020). Principal Parameters Controlling Water Composition in Saline and Brackish Lakes in Eastern Transbaikalia. *Geochem. Int.*, 58, pp. 1356–1373. https://doi.org/10.1134/S0016702920090037

Borzenko S.V. (2021). The main formation processes for different types of salt lakes: Evidence from isotopic composition with case studies of lakes in Transbaikalia, Russia. *Sci. Total Environ.,* 782, 146782. DOI: 10.1016/j.scitotenv.146782

Borzenko S.V., Drebot V.V., Fedorov I.A. (2020). Main formation conditions of soda-type groundwater: A case study from south-eastern Transbaikal region (Russia). *Appl. Geochem*., 123. DOI: 10.1016/j.apgeochem.2020.104763

Borzenko S.V., Fedorov I.A. (2024). Geochemical transformations of sulfur and their role in the formation of different types and subtypes of saline lakes in Southeastern Transbaikalia. *Applied Water Science*, 14, 32. DOI: 10.1007/s13201-023-02082-2

Borzenko S.V., Shvartsev S.L. (2019). Chemical composition of salt lakes in East Transbaikalia (Russia). *Appl. Geochem*., 103, pp. 72–84. https://doi.org/10.1016/j.apgeochem.2019.02.014

Dambaev V.B., Gonchikov G.G., Buryukhaev S.P., Tsyrenov B.S., Zyakun A.M., Namsaraev B.B. (2011). Microbiological and isotopic-geochemical studies in the dry-steppe lakes and saline solonchaks of Western Transbaikalia. *Microbiology*, 80(6), pp. 850–859. https://doi.org/10.1134/S0026261711050031

De Lange G.J., Krijgsman W. (2010). Primary Messinian Salinity Crisis shallow gypsum vs. deep dolomite formation: A unifying biogeochemical mechanism. *Mar. Geol*., 275, pp. 273–277. https://doi.org/10.1016/j.margeo.2010.05.003

Deocampo D.M., Behrensmeyer A.K., and Potts R. (2010). Ultrafine clay minerals of the Pleistocene Olorgesailie Formation, southern Kenya Rift: Diagenesis and paleoenvironments of early hominins. *Clays and Clay Minerals*, 58, pp. 294–310. https://doi.org/10.1346/CCMN.2010.0580301

Deocampo D.M., Cuadros J., Wing-Dudek T., Olives J., and Amouric M. (2009). Saline lake diagenesis as revealed by coupled mineralogy and geochemistry of multiple ultrafine clay phases: Pliocene Olduvai Gorge, Tanzania. *American Journal of Science*, 309, pp. 834–868. https://doi.org/10.2475/09.2009.03

Deocampo D.; Jones B. (2014). Geochemistry of Saline Lakes. In Treatise on Geochemistry. Volume 7: Surface and Groundwater, Weathering, and Soils, 2nd ed.; Drever, J.I., Ed.; Elsevier: Amsterdam, The Netherlands. Chapter 7.13. doi: 10.1016/B978-0-08-095975-7.00515-5

Donchyts G., Baart F., Winsemius H., Gorelick N., Kwadijk J., Van De Giesen N. (2016). Earth's surface water change over the past 30 years. *Nat. Clim Chang*., 6, pp. 810–813. doi: 10.1038/nclimate3111

Erler A.R., Frey S.K., Khader O., d'Orgeville M., Park, Y.-J., Hwang H.-T., Lapen D.R., Peltier W.R., Sudicky E.A. (2018). Simulating Climate Change Impacts on Surface Water Resources Within a Lake-Affected Region Using Regional Climate Projections. *Water Resour. Res*., 55. doi: 10.1029/2018WR024381

Galimov E.M. (1968). Geochemistry of carbon-stable isotopes. Nedra, 226 p. (In Russ.)

Garrels R.M., Christ C.L. (1965). Solutions, Minerals, and Equilibria. Harper and Row, New York, 450 p.

Gaskova O.L., Strakhovenko V.D., Ermolaeva N.I., Zarubina E.Y., Ovdina E.A. (2017). A simple method to model the reduced environment of lake bottom sapropel formation. *Chin. J. Ocean. Limnol.*, 35, pp. 956–966. doi: 10.1007/s00343-017-5345-9

Hardie L.A., Eugster H.P. (1970). The evolution of closed basin brines. *Mineral. Soc. Am.*, 3, pp. 273–290.

Jones B.F., Naftz D.L., Spencer R.J., Oviatt C.G. (2009). Geochemical evolution of Great Salt Lake, Utah, USA. Aquat. *Geochem*., 15, pp. 95–121. doi: 10.1007/s10498-008-9047-y

Jones B.F., Spencer R.J. (1999). Clay mineral diagenesis at Great Salt Lake, Utah, USA. *5th International Symposium on the Geochemistry of the Earth's Surface*, Reykjavik, Iceland, pp. 293–297. Rotterdam: Balkema.

Jones B.F., Naftz D.L., Spencer R.J., and Oviatt C.G. (2009). Geochemical evolution of Great Salt Lake, Utah, USA. *Aquatic Geochemistry*, 15, pp. 95–121. https://doi.org/10.1007/s10498-008-9047-y

Khotinsky N.A. (1977). The Holocene of Northern Eurasia. Moscow: Nauka, 192 p. (In Russ.)

Kolpakova M., Gaskova O., Borzenko S., Krivonogov S., Naymushina O., Rudaya N. (2020). Distribution profile of chemical elements during the last 13 thousand years from the sediments of Maloye Yarovoe lake (Western Siberia, Russia). *Water*, 12(11), 3001. doi: 10.3390/w12113001

Kolpakova M.N., Gaskova O.L., Naymushina O.S., Karpov A.V., Vladimirov A.G., Krivonogov S.K. (2019). Saline lakes of Northern Kkazakhstan: geochemical correlations of elements and controls on their accumulation in water and bottom sediments. *Appl. Geochem*., 107, pp. 8–18. https://doi.org/10.1016/j.apgeochem.2019.05.013

Leonova G.A., Mal'tsev A.E., Melenevskii V.N., Miroshnichenko L.V., Kondrat'eva L.M., Bobrov V.A. (2018). Geochemistry of Diagenesis of Organogenic Sediments: An Example of Small Lakes in Southern West Siberia and Western Baikal Area. *Geochem. Int*., 56, pp. 344–361. doi: 10.1134/S0016702918040043

Maberly S.C., O'Donnell R.A., Woolway R.I, Cutler M.E., Gong M., Jones I.D., Merchant C.J., Miller C.A., Politi E., Marian Scott, E. (2020). Global lake thermal regions shift under climate change. *Nat. Commun*., 11, 1232. doi: 10.1038/s41467-020-15108-z

Maltsev A.E., Krivonogov S.K., Vosel Y.S., Miroshnichenko L.V., Shavekin A.S., Leonova G.A., Solotchin P.A., Bychinsky V.A. (2022). Geochemistry of early diagenesis in sediments of Russian Arctic Glacial lakes (Norilo–Pyasinskaya water system). *Minerals*, 12(4). doi: 10.3390/min12040468

McCaffrey M.A., Lazar B., Holland H.D. (1987). The evapouration path of seawater and the coprecipitation of Br– and K+ with halite. *J. Sedim. Petrol*., 57, pp. 928–937. https://doi.org/10.1306/212F8CAB-2B24-11D7-8648000102C1865D

Mianping Z. (1997). Classification of Saline Lakes and Types of Mineral Deposit. An Introduction to Saline Lakes on the Qinghai—Tibet Plateau; Monographiae Biologicae; Springer: Dordrecht, The Netherlands, 251 p. https://doi.org/10.1007/978-94-011-5458-1

Müller S., Teitz G. (1971). Dolomite replacing "cement A" in biocalcarenites from Fuerteventura, Canary Islands, Spain, in Bricker, D. (ed), Carbonate cements: Johns P. Hopkins University Press, Baltimore, Md., 376 p.

Nordstrom D.K., Ball J.W., Donahoe R.J., Whittemore D. (1989). Groundwater chemistry and water-rock interactions at Stripa. *Geochim. Cosmochim. Acta*, 53(8), pp. 1727–1740. doi: 10.1016/0016-7037(89)90294-9

Obyazov V.A. (2007). Changes in temperature and humidity in the territory of Transbaikalia and neighboring regions of China. Proc. Conf. "Environmental cooperation of the Chita Region (RF) and the Inner Mongolia Autonomous Region (China) in transboundary ecological territories". Chita, pp. 247–250. (In Russ.)

Pačes T. (1983). Rate constants of dissolution derived from the measurements of mass balance in hydrological catchments. *Geochim. Cosmochim. Acta*, 47(11), pp. 1855–1863. doi: 10.1016/0016-7037(83)90202-8

Parkhurst D.L., Appelo C.A. (2013). Description of Input and Examples for PHREEQC Version 3—A Computer Program. for Speciation, Batch-Reaction, One-Dimensional Transport, and Inverse Geochemical Calculations; U.S. Geological Survey Techniques and Methods: Denver, CO, USA, 497 p. https://doi.org/10.3133/tm6A43

Pechenyuk S.I., Semushina Yu.P. (2021). The sorption of ions on the surface of metal oxyhydroxides. SUSU, 243 p. (In Russ.)

Pitzer K.S. (1992). Thermodynamic model of dense aqueous solutions. Thermodynamic modeling in geology: minerals, fluids, melts. Moscow: Mir, pp. 110–153. (In Russ.)

Shvartsev S.L. (1991). Interaction of water with aluminosilicate rocks: review. *Sov. Geol. Geophys*., 32(12), pp. 13–37. (In Russ.)

Shvartsev S.L. (2000). Hydrogeochemistry of hypergenesis zone. *Geochem. Int.*, 28(2), pp. 260–276.

Sklyarov E.V., Vologina E.G., Kulagina N.V., Ukhova N.N., Solotchina E.P., Izokh O.P., Orlova L.A., Solotchin P.A., Stolpovskaya V.N., Sklyarova O.A. (2010). Holocene climate history of the Western Baikal region: carbonate sedimentary record of Hholbo-Nur lake. *Doklady Earth Sciences*, 431(2), pp. 490–496. https://doi.org/10.1134/S1028334X10040173

Solotchin P.A., Solotchina E.P., Zhdanova A.N. (2024). Mineralogy of layered silicates of bottom sediments of high mountain lake Sagan-Nur (Eastern Sayan). *Minerals: structure, properties, research methods*, 14, p. 112. (In Russ.)

Solotchin, P.A., Sklyarov, E.V., Solotchina, E.P. et al. (2017). Carbonate sedimentation in shallow saline lakes of Western Transbaikalia: The response to Holocene climate changes. *Dokl. Earth Sc.,* 473, pp. 461–466. https://doi.org/10.1134/S1028334X17040213

Solotchina E.P. (2009). Structural typomorphism of clay minerals of sedimentary sections and weathering crusts. Novosibirsk: Geo, 234 p. (In Russ.)

Solotchina E.P., Solotchin P.A., Vologina E.G., Sklyarov E.V., Ukhova N.N., Sklyarova O.A. (2013). Holocene sedimentary record of Bol'shoe Alginskoe lake, Western Transbaikalia: connection with paleoclimate. *Doklady Earth Sciences*, 449(1), pp. 313–318. https://doi.org/10.1134/S1028334X13030070

Solotchin P.A., Solotchina E.P., Sklyarov E.V., Strakhovenko V.D., Zhdanova A.N., Danilenko I.V. (2018). Authigenic carbonate formation in small lake basins of Western Transbaikalia. *Bulletin of Transbaikal State University*, 24(6), pp. 45–54. (In Russ.)

Solotchina E.P., Solotchin P.A., Danilenko I.V., Sklyarov E.V., Zamana L.V., Sklyarova O.A., Tat'koy P.G. (2017). Authigenic carbonate sedimentation in Eravnoe group lakes (Western Transbaikalia): response to holocene climate change. *Russian Geology and Geophysics,* 58(11), pp. 1390–1400. https://doi.org/10.1016/j.rgg.2017.11.005

Sonnenfeld P. (1988). Brines and evaporites: Moscow: Mir Publishing House, 480 p. (In Russ.)

Spencer R.J., Hardie L.A. (1990). Control of seawater composition by mixing of river waters and mid-ocean ridge hydrothermal brines, in Spencer, R. J., and Chou, I. M., editors, Fluid-Mineral Interactions: A Tribute to H. P. Eugster: Special Publication 2, The Geochemical Society, pp. 409–449.

Strakhov N.M. (1962). Fundamentals of the theory of lithogenesis. Aphorisms. Moscow: Academy of Sciences of the USSR, 551 p. (In Russ.)

Strakhov N.M. (1993). Selected works. Sedimentation in modern reservoirs. Moscow, Nauka, 396 p. (In Russ.)

Strakhovenko V.D., Shcherbov B.L., Malikova I.N., Vosel' Y. (2010). The regularities of distribution of radionuclides and rear-earth elements in bottom sediments of Siberian lakes. *Russ. Geol. Geophys*., 51, pp. 1167–1178. doi: 10.1016/j.rgg.2010.10.002

Subetto D.A. (2009). Bottom sediments of the lake: paleolimnological reconstructions. St. Petersburg: RSPU Publishing House, 343 p. (In Russ.)

Talbot M.R. (1990). A review of the palaeohydrological interpretation of carbon and oxygen isotope ratios in primary lacustrine carbonates. *Chemical Geology* (Isotope Geoscience Section), 80, pp. 261–279. https://doi.org/10.1016/0168-9622(90)90009-2

Tessier A., Cambell P.G., Bisson M. (1979). Sequential extraction procedure for the speciation of particulate trace metals. *Anal. Chem*., 51, pp. 844–851. https://doi.org/10.1021/ac50043a017

Tweed S., Grace M., Leblanc M., Cartwright I., Smithyman D. (2011). The individual response of saline lakes to a severe drought. *Sci. Total Environ*., 409, pp. 3919–3933. doi: 10.1016/j.scitotenv. 2011.06.023

Velichko A.A. (1989). The Holocene as an element of the global natural process. Paleoclimate of the Late Pleistocene and Holocene. Moscow: Nauka, pp. 5–12. (In Russ.)

Velichko A.A. (2012). Evolutionary geography: problems and solutions. Moscow: GEOS, 564 p. (In Russ.)

Keller W.D. (1963). Geochemistry of lithogenesis. Moscow: Publishing House of Foreign Languages, pp. 85–197. (In Russ.)

Warren J.K. (1989). Evaporite Sedimentology. *J. Sedimentology*, 29(5), pp. 548–556.

Yechieli Y., Wood W.W. (2002). Hydrogeologic processes in saline systems: Playas, sabkhas, and saline lakes. *Earth Sci. Rev*., 58, pp. 343–365. doi: 10.1016/S0012-8252(02)00067-3

Zamana L.V., Oblizov V.A. (2004). Dynamics of the level and hydrochemical regime of the Torey lakes in the twentieth century. Scientific foundations of river basin protection: interdisciplinary approaches to natural resource management: Proc. Ulan-Ude (Russia) – Ulaanbaatar (Mongolia). Ulan-Ude: BNC Publishing House, pp. 98–99. (In Russ.)

Zamana L.V., Ptitsyn A.B., Reshetova S.A., Kalugin I.A., Chu G., Dar'in A.V. (2011). Estimation of modern sedimentation rate in Zun-Torei lake (East Trans-Baikal region) by ^{137}Cs. *Doklady Earth Sciences*, 437(1), pp. 335–339. https://doi.org/10.1134/S1028334X11030287

Zheng M. (2014). Saline lakes and salt basin deposits in China. Beijing: Science Press, 321 p.

About the Authors

Svetlana V. Borzenko – Professor, Chief Researcher, Head of the Laboratory, Institute of Natural Resources, Ecology and Cryology of the Siberian Branch of the Russian Academy of Sciences

16a, Nedorezova Av., Chita, 672014, Russian Federation

e-mail: svb_64@mail.ru

Irina A. Komogortseva – Junior Researcher, Institute of Natural Resources, Ecology and Cryology of the Siberian Branch of the Russian Academy of Sciences

16a, Nedorezova Av., Chita, 672014, Russian Federation

e-mail: komogorcevai@bk.ru

Manuscript received 15 January 2025;
Accepted 1 August 2025; Published 30 March 2026

Основные механизмы эволюции озер Хилганта и Горбунка (Юго-Восточное Забайкалье)

С.В. Борзенко, И.А. Комогорцева*
Институт природных ресурсов, экологии и криологии Сибирского отделения РАН, Чита, Россия
**Ответственный автор: Светлана Владимировна Борзенко, e-mail: svb_64@mail.ru*

В статье рассматривается гидрогеохимическая история континентальных соленых, хлоридных озер Хилганта и Горбунка, расположенных на юго-востоке Забайкалья. Анализируются химический состав, pH, соленость, величины соотношения генетических коэффициентов rMg/rCa и rSr/rCa озерных вод в разные годы их опробования. Выделяются основные связи солености с содержанием макрокомпонентов озерных вод. Приводятся краткие сведения о минеральном и химическом составах водовмещающих пород и химическом составе воды, участвующей в солевом питании озер. Описываются минеральный и химический составы, значения изотопного соотношения углерода и кислорода карбонатов в разных слоях донных осадков озер. Выделяются минералы-индикаторы, характеризующие разные климатические обстановки. Определяются основные условия, характеризующие содержания и величины соотношения основных химических компонентов и pH, в период изменения солености озерных вод. На основе измерений ^{210}Pb рассчитываются возраст и современная скорость накопления осадков в озерах. Анализируются термодинамические расчеты в системе «вода – горная порода» при разных температурах воды. Рассматриваются физико-химические условия образования аутигенных и хемогенных минералов. В конечном счете, интерпретируется геохимическая эволюция озер в связи с региональными изменениями климата в недавнем прошлом.

Ключевые слова: соленые озера, аутигенные и хемогенные минералы, изотопы, испарение, эволюция

Для цитирования: Борзенко С.В., Комогорцева И.А. (2026). Основные механизмы эволюции озер Хилганта и Горбунка (Юго-Восточное Забайкалье). *Георесурсы,* 28(1), с. 160–176. https://doi.org/10.18599/grs.2026.1.7